

AD-A206 458

# Attenuation Measurement of Very Low-Loss Dielectric Waveguides by the Cavity Resonator Method in the Millimeter/Submillimeter Wavelength Range

F. I. SHIMABUKURO  
Electronics Research Laboratory  
Laboratory Operations  
The Aerospace Corporation  
El Segundo, CA 90245

and

C. YEH  
Department of Electrical Engineering  
University of California  
Los Angeles, CA 90024

20 March 1989

Prepared for  
SPACE DIVISION  
AIR FORCE SYSTEMS COMMAND  
Los Angeles Air Force Base  
P.O. Box 92960  
Los Angeles, CA 90009-2960

DTIC  
ELECTE  
3 APR 1989  
S D  
E

APPROVED FOR PUBLIC RELEASE;  
DISTRIBUTION UNLIMITED

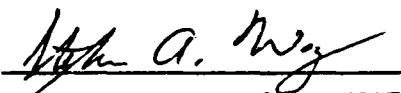
89 4 03 071

This report was submitted by The Aerospace Corporation, El Segundo, CA 90245, under Contract No. F04701-85-C-0086-P00019 with the Space Division, P.O. Box 92960, Los Angeles, CA 90009-2960. It was reviewed and approved for The Aerospace Corporation by M. J. Daugherty, Director, Electronics Research Laboratory.

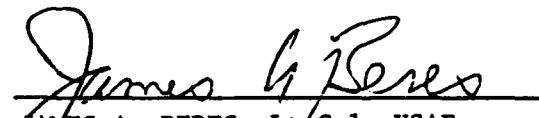
Lt. Stephen A. Way was the project officer for the Mission-Oriented Investigation and Experimentation (MOIE) Program.

This report has been reviewed by the Public Affairs Office (PAS) and is releasable to the National Technical Information Service (NTIS). At NTIS, it will be available to the general public, including foreign nationals.

This technical report has been reviewed and is approved for publication. Publication of this report does not constitute Air Force approval of the report's findings or conclusions. It is published only for the exchange and stimulation of ideas.



STEPHEN A. WAY, 2Lt, USAF  
MOIE Project Officer  
AFSTC/WCO OL-AB



JAMES A. BERES, Lt Col, USAF  
Director, AFSTC, West Coast Office  
AFSTC/WCO OL-AB

SECURITY CLASSIFICATION OF THIS PAGE

## REPORT DOCUMENTATION PAGE

1a REPORT SECURITY CLASSIFICATION <b>Unclassified</b>			1b RESTRICTIVE MARKINGS			
2a SECURITY CLASSIFICATION AUTHORITY			3. DISTRIBUTION / AVAILABILITY OF REPORT Approved for public release; distribution unlimited.			
2b DECLASSIFICATION / DOWNGRADING SCHEDULE						
4. PERFORMING ORGANIZATION REPORT NUMBER(S) TR-0086A(2925-06)-1			5 MONITORING ORGANIZATION REPORT NUMBER(S) SD-TR-89-10			
6a. NAME OF PERFORMING ORGANIZATION The Aerospace Corporation Laboratory Operations		6b OFFICE SYMBOL (If applicable)	7a. NAME OF MONITORING ORGANIZATION Space Division			
6c. ADDRESS (City, State, and ZIP Code) El Segundo, CA 90245			7b ADDRESS (City, State, and ZIP Code) Los Angeles Air Force Base Los Angeles, CA 90009-2960			
8a. NAME OF FUNDING / SPONSORING ORGANIZATION		8b OFFICE SYMBOL (If applicable)	9 PROCUREMENT INSTRUMENT IDENTIFICATION NUMBER F04701-85-C-0086-P00019			
8c. ADDRESS (City, State, and ZIP Code)			10 SOURCE OF FUNDING NUMBERS			
			PROGRAM ELEMENT NO.	PROJECT NO.	TASK NO.	WORK UNIT ACCESSION NO.
11 TITLE (Include Security Classification) Attenuation Measurement of Very Low-Loss Dielectric Waveguides by the Cavity Resonator Method in the Millimeter/Submillimeter-Wavelength Range						
12. PERSONAL AUTHOR(S) Shimabukuro, F. I. and Yeh, C.						
13a. TYPE OF REPORT		13b TIME COVERED FROM _____ TO _____		14. DATE OF REPORT (Year, Month, Day) 1989 March 20		15 PAGE COUNT 33
16 SUPPLEMENTARY NOTATION						
17. COSATI CODES			18 SUBJECT TERMS (Continue on reverse if necessary and identify by block number)			
FIELD	GROUP	SUB-GROUP	Attenuation measurement of low-loss dielectric waveguides			
			Determination of complex permittivity of materials			
			Dielectric waveguides			
19. ABSTRACT (Continue on reverse if necessary and identify by block number)						
<p>A dielectric waveguide shorted at both ends is constructed as a cavity resonator. By measuring the Q of this cavity, one can determine the attenuation constant of the guided mode on this dielectric structure. The complex permittivity of the dielectric waveguide material can also be derived from these measurements. Measurements were made at Ka-band for dielectric waveguides constructed of nonpolar, low-loss polymers such as Teflon, polypropylene, polyethylene, polystyrene, and Rexolite.</p>						
20 DISTRIBUTION / AVAILABILITY OF ABSTRACT <input checked="" type="checkbox"/> UNCLASSIFIED/UNLIMITED <input type="checkbox"/> SAME AS RPT <input type="checkbox"/> DTIC USERS			21 ABSTRACT SECURITY CLASSIFICATION Unclassified			
22a NAME OF RESPONSIBLE INDIVIDUAL			22b TELEPHONE (Include Area Code)		22c OFFICE SYMBOL	

PREFACE

The authors thank H. B. Dyson for his invaluable help in setting up the experiment and making the measurements, and G. G. Berry for fabricating the Fabry-Perot plates and the dielectric waveguides. C. Yeh thanks Dr. Jim Hamada and Dr. Bill Wong for their enthusiastic support of the UCLA-TRW MICRO Program.

Accession For	
NTIS (GSA&I)	<input checked="" type="checkbox"/>
DTIC TAB	<input type="checkbox"/>
Unannounced	<input type="checkbox"/>
Justification	
By _____	
Distribution/	
Availability Codes	
Dist	Avail and/or Special
A-1	



## CONTENTS

PREFACE.....	1
I. INTRODUCTION.....	5
II. THEORETICAL FOUNDATION.....	7
III. ULTRAHIGH-Q DIELECTRIC-ROD RESONANT CAVITY.....	11
IV. EXPERIMENTAL RESULTS.....	23
REFERENCES.....	33

## FIGURES

1.	Schematic of the Dielectric Waveguide Cavity Resonator, Including the Measurement Setup.....	8
2.	Dispersion of the $HE_{11}$ Mode of a Dielectric Rod Waveguide of Radius $a$ .....	10
3.	$\omega$ versus $\beta$ for Several Propagating Modes Along a Dielectric Waveguide.....	17
4.	Power Output of a Swept Input Signal Through a Dielectric Waveguide in a Parallel-Plate Resonator.....	18
5.	Plots of the Attenuation Factor $R$ in a Circular Dielectric Waveguide of Radius $a$ for Different Relative Permittivities.....	21
6.	Photograph of the Output on the Spectrum Analyzer Through the Dielectric Waveguide in the Parallel-Plate Cavity at a Transmission Resonance.....	24
7.	Measured $Q$ 's of the Different Circular Dielectric Waveguides.....	25
8.	Comparison of Measured and Calculated Group and Phase Velocities for a Teflon Rod Waveguide of Diameter 0.635 cm.....	26
9.	Derived Values of $\epsilon_r$ and $\tan\delta$ from the Measurements for Different Dielectric Materials.....	27
10.	Measured Attenuation Coefficients for the Different Dielectric Waveguides Corresponding to Fig. 9.....	29
11.	Plot of Half-Power Transmission Bandwidths at the Different Resonances for Two Different Lengths of Circular Teflon Waveguide.....	30
12.	Comparison of Attenuation Coefficients for Silver Rectangular and Teflon Circular Waveguides at the Indicated Frequencies.....	32

## TABLE

1.	Measured Relative Permittivities and Loss Tangents, Ka-Band.....	28
----	--	----

## I. INTRODUCTION

By using a specially configured dielectric rod made from low-loss, non-polar polymers, one can construct millimeter/submillimeter dielectric waveguides that support the dominant mode with a very small attenuation coefficient. To verify experimentally the low-loss characteristics of such waveguides, an accurate measurement scheme must be devised. A logical solution is to construct a cavity consisting of a length of a dielectric-rod waveguide that supports the mode of interest, with parallel shorting plates at both ends.<sup>1</sup> At a resonant frequency of such a cavity, the guide wavelength  $\lambda_g$  is obtained from the cavity spacing, and the attenuation constant  $\alpha$  can be obtained from the measured Q. This cavity method also provides an accurate determination of the dielectric properties of the waveguide material.

This report describes the theoretical foundation for this cavity technique. Then, a detailed discussion and derivation of the relationship between  $\alpha$  and Q are given. Finally, experimental results for several low-loss dielectric materials are presented.



## II. THEORETICAL FOUNDATION

The geometry of a dielectric rod resonator, including a schematic of the measurement system, is shown in Fig. 1. The signals are coupled in and out of the resonator through small coupling holes in the center of the reflecting plates. For a circular step-index dielectric rod, the  $HE_{11}$  mode is the dominant guided mode for this dielectric waveguide.<sup>2,3</sup> The longitudinal fields of this  $HE_{11}$  mode resonate between two shorting, parallel plates, and are given by the following:

Inside the core region ( $\rho < a$ ),

$$E_{zi} = A J_1(u\rho) \sin\phi \cos\beta z \quad (1)$$

$$H_{zi} = B J_1(u\rho) \cos\phi \sin\beta z \quad (2)$$

$$u^2 = k_1^2 - \beta^2, \quad k_1^2 = \omega^2 \mu \epsilon_1 \quad (3)$$

and

$$\beta = \frac{m\pi}{d}, \quad m = 1, 2, 3 \dots$$

Outside the core region ( $\rho > a$ ),

$$E_{zo} = C K_1(w\rho) \sin\phi \cos\beta z \quad (4)$$

$$H_{zo} = D K_1(w\rho) \cos\phi \sin\beta z \quad (5)$$

with

$$w^2 = \beta^2 - k_2^2, \quad k_2^2 = \omega^2 \mu \epsilon_2 \quad (6)$$

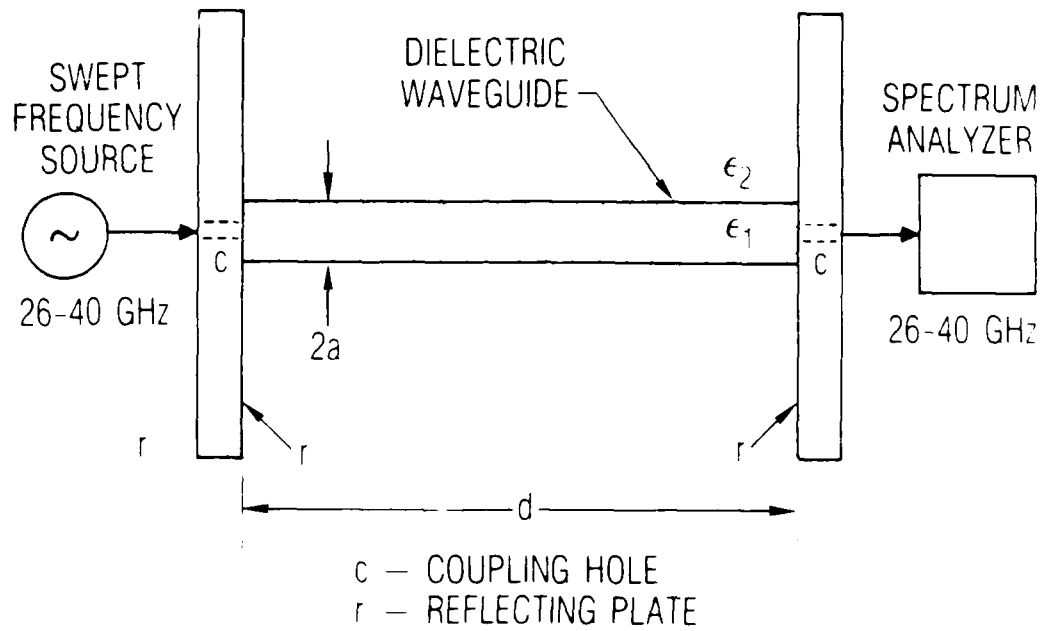


Fig. 1. Schematic of the Dielectric Waveguide Cavity Resonator, Including the Measurement Setup

In the previous equations, A, B, C, and D are arbitrary constants;  $J_1(u\rho)$  is the Bessel function;  $K_1(w\rho)$  is the modified Bessel function;  $a$  is the radius of the dielectric rod;  $d$  is the spacing between the shorting plates;  $\epsilon_1$  and  $\epsilon_2$  are the permittivities of the regions inside and outside the core, respectively;  $\omega$  is the angular frequency of the resonant mode; and  $\mu = \mu_0$  is the permeability of free space. In this study the region outside the core is free space and  $\epsilon_2 = \epsilon_0$ . Note that all the transverse fields ( $E_\phi$ ,  $E_\rho$ ,  $H_\phi$ ,  $H_\rho$ ), may be derived from the longitudinal fields ( $E_z$  and  $H_z$ ).<sup>4</sup> By satisfying the boundary conditions at  $\rho = a$ , the following dispersion relation is obtained:

$$\left[ \frac{J_1'(ua)}{uJ_1(ua)} + \frac{K_1'(wa)}{wK_1(wa)} \right] \left[ \frac{k_1^2 J_1(ua)}{uJ_1(ua)} + \frac{k_0^2 K_1'(wa)}{wK_1(wa)} \right] = \left(\frac{\beta}{a}\right)^2 \left[ \frac{1}{u^2} + \frac{1}{w^2} \right]^2 \quad (7)$$

The solution of this dispersion relation will yield the guide wavelength ( $\lambda_g = \frac{2\pi}{\beta}$ ) of the cavity for the  $HE_{11}$  mode for a given  $a$ ,  $d$ ,  $\epsilon_1/\epsilon_0$ ,  $\mu_0$ , and  $\omega$ . Results for various values of  $\epsilon_r (= \epsilon_1/\epsilon_0)$  are shown in Fig. 2.

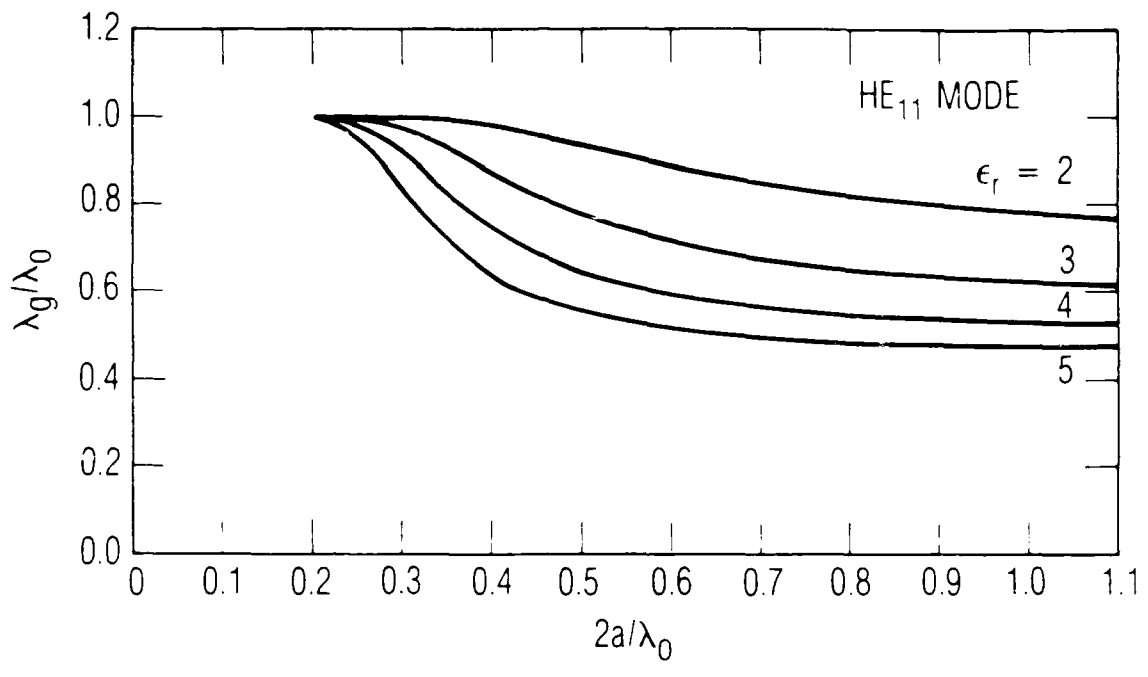


Fig. 2. Dispersion of the HE<sub>11</sub> Mode of a Dielectric Rod Waveguide of Radius a. The solution is given as a plot of the normalized guide wavelength as a function of normalized rod diameter.  $\lambda_0$  is the free-space wavelength.

### III. ULTRAHIGH-Q DIELECTRIC-ROD RESONANT CAVITY

As shown in Fig. 1, a dielectric-rod resonant cavity consists of a dielectric waveguide of length  $d$  terminated at its ends by sufficiently large, flat, and highly reflecting plates that are perpendicular to the axis of the guide. Microwave energy is coupled into and out of the resonator through small coupling holes at both ends of the cavity. For best results, the holes are dimensioned such that they are beyond cutoff. At resonance the length  $d$  of the cavity must be  $m\lambda_g/2$  ( $m$  is an integer), where  $\lambda_g$  is the guide wavelength of the particular mode under consideration. By measuring the resonant frequency of the cavity, one may obtain the guide wavelength of that particular guided mode in the dielectric waveguide. The propagation constant  $\beta$  of that mode is related to  $\lambda_g$  and  $v_p$ , the phase velocity, as follows:

$$\beta = \frac{2\pi}{\lambda_g} = \frac{\omega}{v_p} \quad (8)$$

The  $Q$  of a resonator is indicative of the energy storage capability of a structure relative to the associated energy dissipation arising from various loss mechanisms, such as those due to the imperfection of the dielectric material and the finite conductivity of the end plates. The common definition for  $Q$  is applicable to the dielectric-rod resonator, and is given by

$$Q = \omega \frac{\bar{W}}{\bar{P}} \quad (9)$$

where  $\omega$  is the angular frequency of oscillation,  $\bar{W}$  is the total time-averaged energy stored, and  $\bar{P}$  is the average power loss.

For the case under study, with carefully machined dielectric rods and proper cavity alignment, the time-averaged power dissipation  $\bar{P}$  consists of two parts, the power loss due to the dielectric rod and that due to the metal end walls, namely,

$$\bar{P} = \bar{P}_{\text{dielectric}} + \bar{P}_{\text{wall}}$$

The power dissipation due to the dielectric rod is given by

$$\bar{P}_{\text{dielectric}} = \frac{1}{2} \sigma_d \int_0^d \int_{A_d} (\underline{E}_1 \cdot \underline{E}_1^*) dA dz \quad (10)$$

where  $\underline{E}_1$  is the electric field within the dielectric rod,  $\sigma_d$  is the conductivity of the dielectric,  $A_d$  is the cross-sectional area of the dielectric rod, and the asterisk denotes the complex conjugate. The loss due to both end walls is given by

$$\bar{P}_{\text{wall}} = 2 \left( \frac{R_s}{2} \right) \int_{A_w} (\underline{H}_t \cdot \underline{H}_t^*) dA \quad (11)$$

where  $R_s = \sqrt{\frac{\omega \mu}{2\sigma_r}}$ , the wall surface resistivity;  $\sigma_r$  is the conductivity of the reflector material; and  $\underline{H}_t$  is the tangential component of the magnetic field along the metal wall. Here,  $A_w$  is the area of each conducting wall. There is also a loss due to the coupling hole; however, as in this experiment, the coupling can be made small enough that the primary wall losses can be considered to be the ohmic wall losses. Thus

$$\bar{W} = 2 \bar{W}_m = 2 \bar{W}_e = \mu \int_V (\underline{H} \cdot \underline{H}^*) dV = \epsilon \int_V (\underline{E} \cdot \underline{E}^*) dV \quad (12)$$

where  $V$  is the total volume of the cavity,  $\bar{W}_m$  and  $\bar{W}_e$  are the time-averaged magnetic and electric energies, respectively, and  $\underline{H}$  and  $\underline{E}$  are the total fields. Equations (9) through (12) can be rearranged to obtain

$$\frac{1}{Q} = \frac{\bar{P}}{\omega \bar{W}} = \frac{\bar{P}_{\text{dielectric}}}{\omega \bar{W}} + \frac{\bar{P}_{\text{wall}}}{\omega \bar{W}} = \frac{1}{Q_d} + \frac{1}{Q_w} \quad (13)$$

The term  $Q_d$  is the Q factor of the cavity if the end plates were perfectly conducting, and  $Q_w$  is the Q factor of the cavity if the dielectric were perfect. From Eq. (13) we have

$$Q_d = \frac{\omega \bar{W}}{P_{\text{dielectric}}} = \frac{1}{2 \tan \delta} \frac{C_T}{C_D} \quad (14)$$

$$Q_w = \frac{\omega \bar{W}}{P_{\text{wall}}} = \frac{d}{2\delta_r} \frac{C_T}{C_W} \quad (15)$$

where  $\tan \delta = \frac{\sigma}{\omega \epsilon_1}$  is the loss tangent of the dielectric rod, and  $\delta_r = \frac{2R}{\omega \mu}$  is the skin depth of the metallic end plates. The ratios  $C_T/C_D$  and  $C_T/C_W$  are dimensionless quantities involving integrals of the fields.

Note that  $Q_d$  is independent of the length of the cavity, whereas  $Q_w$  is proportional to the length. For a long cavity,  $Q_w \gg Q_d$ , and  $Q = Q_d$ . By measuring the Q of the cavity with  $Q_w \gg Q_d$ , one can obtain the attenuation constant  $\alpha$  of the given mode.

In 1944 Davidson and Simmonds<sup>5</sup> derived a relationship between the Q of a cavity composed of a uniform transmission line with short-circuiting ends and the attenuation constant  $\alpha$  of such a transmission line. In 1950 Barlow and Cullen<sup>6</sup> rederived this relationship. The latter authors showed that this relationship is quite general and is applicable to uniform metal-tube waveguides having arbitrary cross section. Since then, one of the standard techniques for measuring the attenuation constant  $\alpha$  is the use of the cavity method.<sup>a</sup> This method is excellent for measuring the attenuation constant of

---

<sup>a</sup>The procedures of this method in general are the following: Short circuit the uniform transmission line under consideration at both ends and measure the Q of such a resonator. From the knowledge of the measured Q and other constants, such as the cut-off frequency of the guide, the frequency of oscillation, etc., it is easy to obtain from the formula derived by these authors.

the guide when the loss is quite small. Later, various authors<sup>1,7</sup> generalized this method and applied it to open waveguides, such as the single wire line, the dielectric cylinder guide, and associated guides.

However, it should be remembered that the formula of Davidson and Simmonds<sup>5</sup> and Barlow and Cullen<sup>6</sup> is derived under the assumption that there exists a single equivalent transmission line for the mode under consideration. This assumption is true for a pure TE, TM, or TEM mode, but it is not clear that such a single equivalent transmission line exists for the hybrid waves. This suspicion arises from the fact that (1) the TE and TM waves are intimately coupled to each other, and (2) the characteristic impedance defined by Schelkunoff<sup>8</sup> is not constant with respect to the transverse coordinates. It is, therefore, very difficult to conceive that there exists a single equivalent transmission line for this hybrid mode; at best the hybrid wave may be represented by a set of transmission lines coupled tightly with one another. Hence, the formula of Davidson and Simmonds and Barlow and Cullen is not applicable to the hybrid wave.<sup>b</sup>

A more general relation between  $Q$  and  $\alpha$  can be obtained without using the transmission-line equivalent circuit, provided that  $\alpha$  is very small compared with  $\beta$ . The propagation constant of a guided wave with a small attenuation constant at  $\omega$  is

$$\Gamma(\omega) = \alpha(\omega) + j\beta(\omega) \quad j = \sqrt{-1} \quad (16)$$

It can be shown that for a waveguide placed between reflecting parallel plates, with miniscule coupling to external circuits,

$$P_t = \frac{1}{|1 - r^2 \exp(-2\Gamma d)|^2} \quad (17)$$

<sup>b</sup>Several investigators, apparently unaware of this restriction, used this formula in their investigations of the hybrid wave.

where  $P_t$  is the power transmission of the resonator,  $r$  is the reflection coefficient at each wall,  $\Gamma$  is the propagation constant [given in Eq. (16)], and  $d$  is the distance between the reflecting plates. At the half-power transmission points,

$$P_t(\omega = \omega_0) = 2 P_t(\omega = \omega_0 \pm \Delta\omega) \quad (18)$$

and

$$\begin{aligned} \beta &= \beta_0 + \Delta\beta \\ \alpha &= \alpha_0 + \Delta\alpha \end{aligned} \quad (19)$$

For the case  $r = 1$  and  $ad \ll 1$ , and using Eqs. (17) through (19), one gets, noting that  $\cos 2\beta d = 1$  (the resonance condition),

$$\Delta\beta \approx \alpha \quad (20)$$

Since

$$\Delta\beta \approx \frac{\partial\beta}{\partial\omega} \Delta\omega, \quad v_p = \frac{\omega}{\beta}, \quad v_g = \frac{\partial\omega}{\partial\beta}, \quad \text{and} \quad Q = \frac{\omega_0}{2\Delta\omega}$$

we finally arrive at the relation

$$\alpha = \frac{\omega_0}{2Qv_g} = \frac{v_p}{v_g} \frac{\beta}{2Q} \quad (21)$$

This is the general relation that we are seeking. This result was also obtained by Yeh,<sup>9</sup> who used an alternative approach. Substituting the values of  $v_p/v_g$  for TE, TM, or TEM into Eq. (21), one gets the relations derived by Davidson et al. For the TM or TE mode,

$$\frac{v_p}{v_g} = \frac{1}{1 - \left(\frac{\lambda}{\lambda_c}\right)^2}, \quad \alpha = \frac{1}{1 - \left(\frac{\lambda}{\lambda_c}\right)^2} \frac{\beta}{2Q}$$

and for the TEM mode,

$$v_p/v_g = 1, \quad \alpha = \beta/2Q$$

where  $\lambda_c$  is the cut-off wavelength.

The group and phase velocity of the dominant modes can be obtained easily from the  $\omega$ - $\beta$  diagram. A sketch of the  $\omega$ - $\beta$  diagram for the propagating modes is shown in Fig. 3. It can be seen that at low frequencies or small  $\beta$ 's,  $v_p \approx v_g$ ; again, at very high frequencies or large  $\beta$ 's,  $v_p \approx v_g$ . Therefore, the relation  $\alpha = \beta/2Q$  is applicable only at very low frequencies or at very high frequencies.

Returning now to the problem of measuring the attenuation constant of very low-loss dielectric waveguides, one notes that by using the dielectric waveguide cavity technique, a Q of the order of 30,000 can readily be measured. At the higher frequencies this value of Q corresponds to a loss tangent of the order of  $10^{-5}$ . A schematic of the experiment is shown in Fig. 1. A dielectric-rod waveguide is placed in a parallel-plate cavity, and a swept signal frequency is transmitted through the waveguide cavity and detected by a spectrum analyzer. The signals are coupled through very small holes in the circular gold-plated reflectors. The plates are large enough (6 in. diam) that the fields beyond the plate diameter are insignificant. The output is a series of narrow transmission resonances at  $f_1, f_2, \dots, f_m$ , with half-power bandwidths  $\Delta f_1, \Delta f_2, \dots, \Delta f_m$ , respectively (see Fig. 4). At each resonant frequency the guide wavelength is given by

$$\lambda_{gm} = \frac{2d}{m} \quad (22)$$

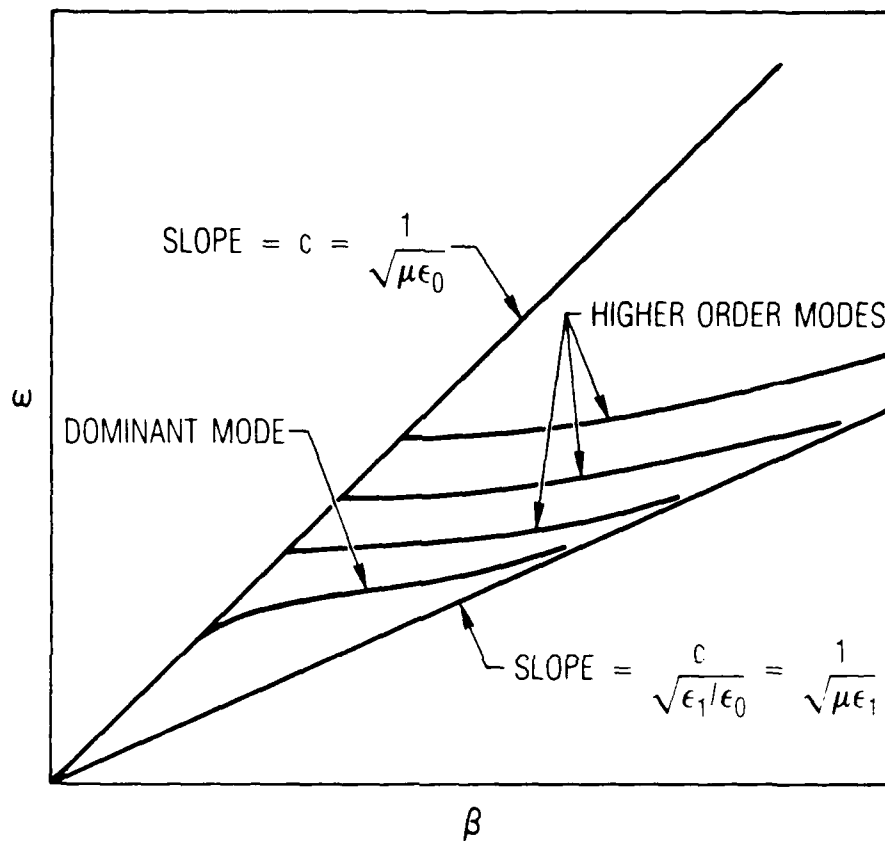


Fig. 3.  $\omega$  versus  $\beta$  for Several Propagating Modes Along a Dielectric Waveguide

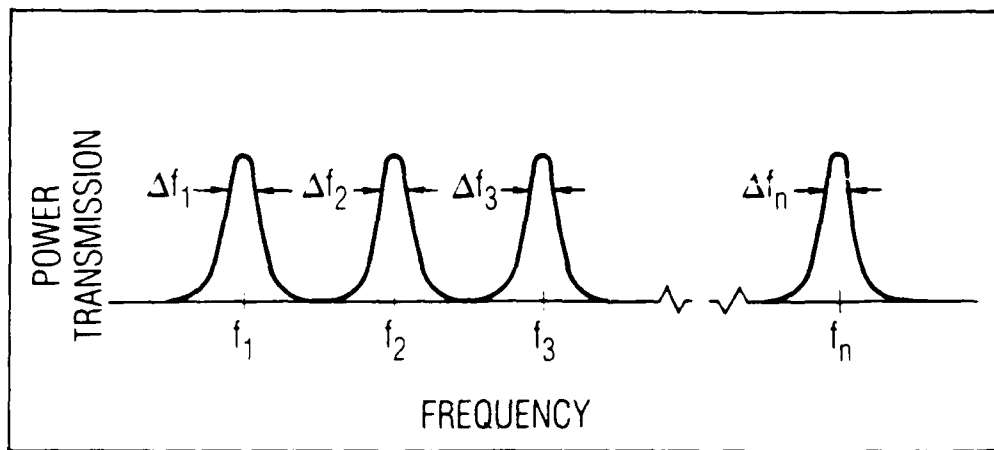


Fig. 4. Power Output of a Swept Input Signal Through a Dielectric Waveguide in a Parallel-Plate Resonator

and the Q by

$$Q_m = \frac{f_m}{\Delta f_m} \quad (23)$$

where  $d$  is the length of the waveguide and  $m$  is the  $m^{\text{th}}$  resonance. The integer  $m$  is the number of guide half-wavelengths at a particular resonant frequency. From  $a$  (the dielectric rod radius), the spacing  $d$ , the guide wavelength  $\lambda_g$ , and the number  $m$ , one can determine the relative dielectric constant  $\epsilon_r = \epsilon_1/\epsilon_0$  at the different frequencies by using the solutions of Eq. (7).

With careful alignment of the waveguide and the shorting plates, the primary loss mechanisms to be considered are the wall losses and the dielectric loss. From previous discussion,

$$\frac{1}{Q_m} = \frac{1}{Q_d} + \frac{1}{Q_w} \quad (24)$$

where  $Q_m$  is the measured Q of the  $m^{\text{th}}$  mode (we recall that  $Q_d$  is independent of cavity length, whereas  $Q_w$  is proportional to cavity length). For the different dielectric waveguides used in this study, the calculated  $Q_w$  ranges from 18000 to 21000  $d$ , where  $d$  is the length in cm. Experimentally, the effect of the wall losses on the cavity Q, whether due to the coupling or to the ohmic dissipation, could not be detected; therefore,

$$Q_w \gg Q_d \quad (25)$$

The measurement verification of Eq. (25) will be discussed in the next section.

The general relation [given in Eq. (21)] between Q and  $\alpha$  for a short-circuited low-loss waveguide is rewritten as

$$\alpha = 8.686 \frac{v_p}{v_g} \frac{\beta}{2Q} \quad (\text{dB/m}) \quad (26)$$

where  $v_p = \omega/\beta$  and  $v_g = d\omega/d\beta$ . It has been shown that, for a dielectric rod waveguide,<sup>10</sup>

$$\alpha = 4.343 \omega \sqrt{\mu \epsilon_0} \tan \delta \epsilon_r R \quad (27)$$

where

$$R = \left| \frac{\int_{A_d} (\underline{E}_1 \cdot \underline{E}_1^*) dA}{\sqrt{\mu \epsilon_0} \int_A \underline{e}_z \cdot (\underline{E} \times \underline{H}^*) dA} \right| \quad (28)$$

As before,  $\epsilon_r = \epsilon_1/\epsilon_0$ ,  $A_d$  is the cross-sectional area of the core region of the dielectric waveguide,  $A$  is the total cross-sectional area,  $\underline{E}_1$  is the electric field within the dielectric rod,  $\underline{e}_z$  is the unit vector along the direction of propagation, and  $\underline{E}$  and  $\underline{H}$  are the total fields. The quantity  $R$  is a frequency-dependent geometrical factor that can be computed. The loss tangent can be obtained by combining Eqs. (26) and (27):

$$\tan \delta = \frac{\frac{v_p}{v_g} \frac{\beta}{Q}}{\omega \sqrt{\mu \epsilon_0} \epsilon_r R} \quad (29)$$

For a circular dielectric waveguide, one can calculate  $R$  for different values of  $\epsilon_r$ . This is shown in Fig. 5. Hence, by measuring the  $Q$  of a dielectric rod in a parallel-plate resonator, the loss tangent of the dielectric and the attenuation constant for the corresponding mode can be obtained. This scheme provides an extremely accurate way of measuring the electrical properties ( $\epsilon_r$ ,  $\tan \delta$ ) of ultralow-loss dielectrics as well as the low attenuation constant for a dielectric waveguide supporting the dominant mode.

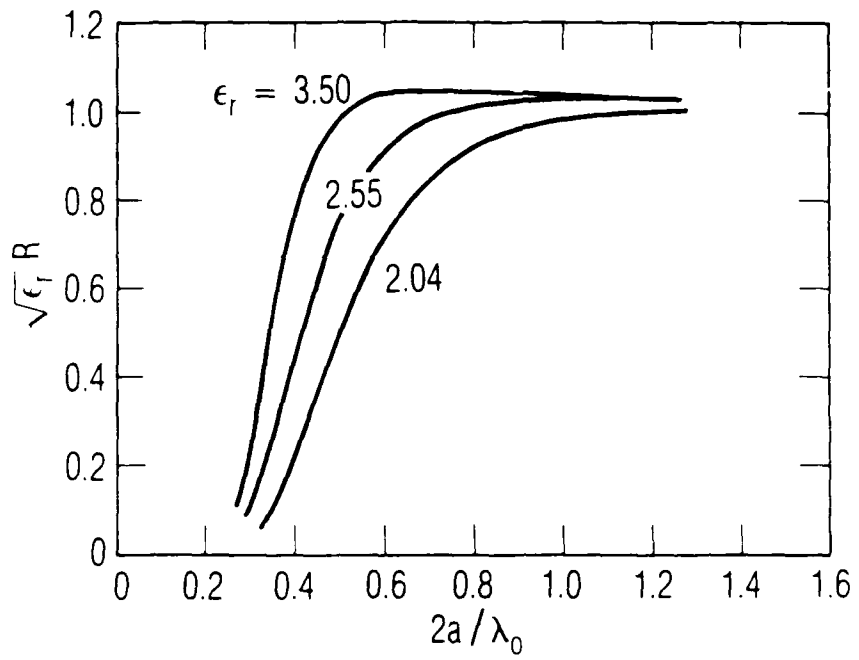


Fig. 5. Plots of the Attenuation Factor R in a Circular Dielectric Waveguide of Radius a for Different Relative Permittivities



#### IV. EXPERIMENTAL RESULTS

Circular dielectric rod waveguides were made of Teflon, Rexolite, polystyrene, polyethylene, and polypropylene. The diameters ranged from 0.4 to 0.63 cm, and the lengths from 15.2 to 20.3 cm. These waveguides were placed in a parallel-plate resonator. A swept frequency signal at Ka-band (26.5 to 40 GHz) was coupled into the resonator and the output was detected by a spectrum analyzer. The input and output coupling was done through a small hole (1.5 mm diam) in an iris in WR-28 waveguide. With this coupling only the  $HE_{11}$  dominant mode was excited. This was verified by mapping the fields outside the dielectric waveguide with an electric probe. A sample measurement of the transmission resonance on the spectrum analyzer is shown in Fig. 6, for a Teflon rod waveguide.

At each resonance the  $Q$  was measured; the results are shown in Fig. 7. Because  $m$  is known to be an integer, one can determine it by measuring the guide wavelength approximately with a probe. Once  $m$  is known, the guide wavelengths at the various resonant frequencies can be accurately determined, the  $\omega$ - $\beta$  diagram can be generated, and  $\alpha$  can be determined from Eq. (26). In this investigation the dielectric waveguides had a circular cross section and the following procedure was used. Once the wavelength and dimensions of the waveguide were known,  $\epsilon_r$  was determined from Eq. (7). From the value of  $\epsilon_r$  for Teflon in Table 1,  $v_p$  and  $v_g$  can be calculated from Eq. (7), for a rod diameter of 0.635 cm. The comparison between the calculated and measured values of  $v_p$  and  $v_g$  are shown in Fig. 8. The measured group velocity was obtained by assuming a linear relation between adjacent measured values on the  $\omega$ - $\beta$  curve. The attenuation coefficient was calculated from Eq. (26) and  $\tan\delta$  was obtained from Eq. (29). The field configurations for the circular waveguide were known, and  $\tan\delta$  was also calculated from Eq. (14), which gave the same results as Eq. (29).

The measured relative permittivities and loss tangents at different resonant frequencies for the materials above are shown in Fig. 9. The average values with the corresponding standard deviations are given in Table 1. A

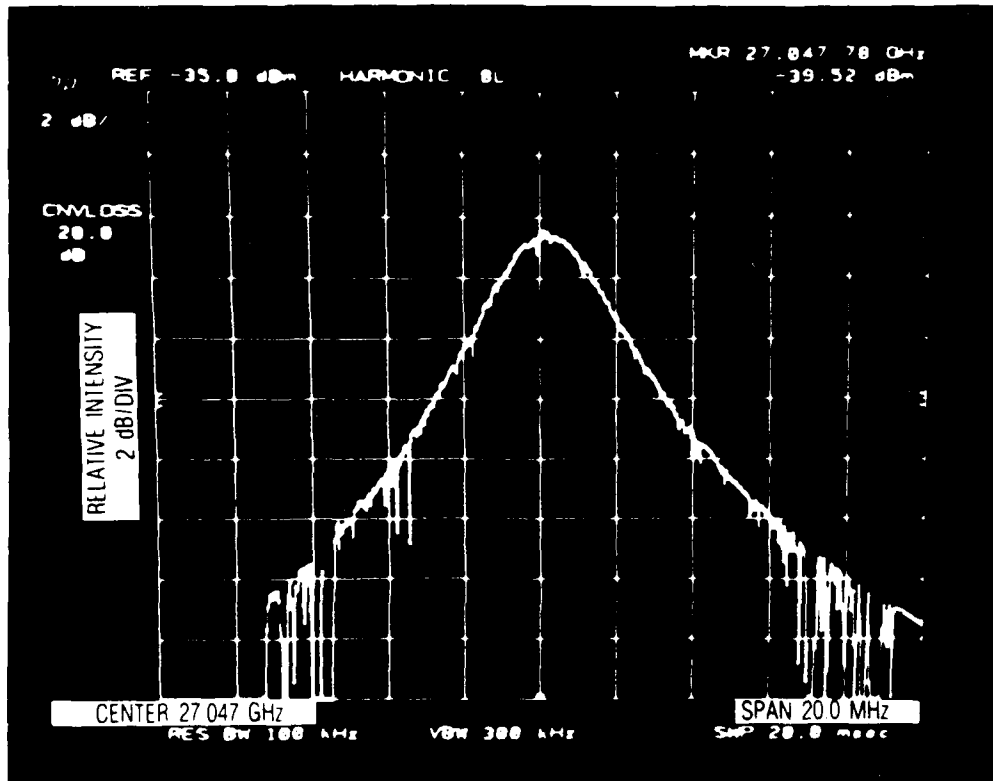


Fig. 6. Photograph of the Output on the Spectrum Analyzer Through the Dielectric Waveguide in the Parallel-Plate Cavity at a Transmission Resonance

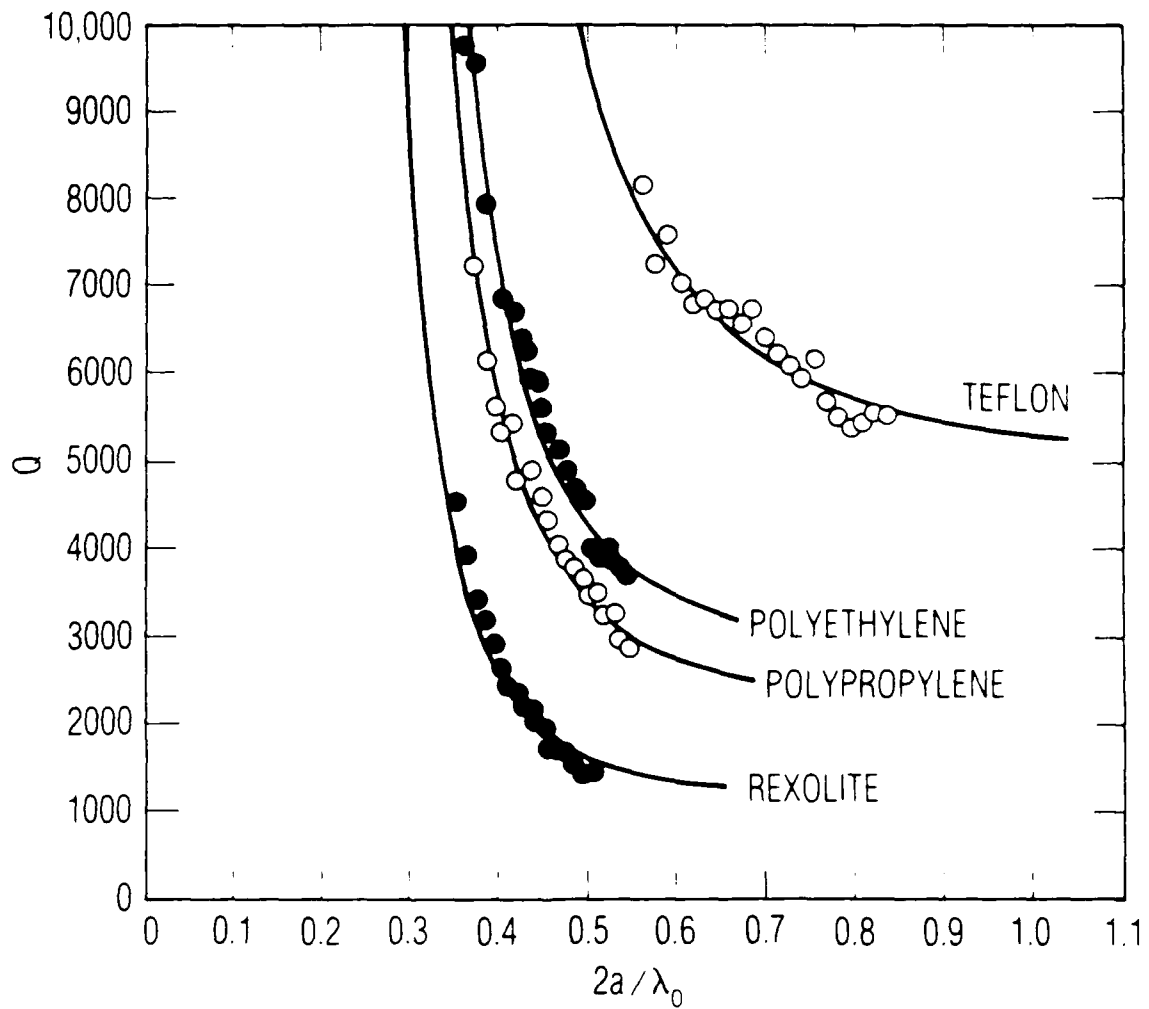


Fig. 7. Measured  $Q$ 's of the Different Circular Dielectric Waveguides. The solid line is the theoretical  $Q_d$  curve using the permittivities given in Table 1.

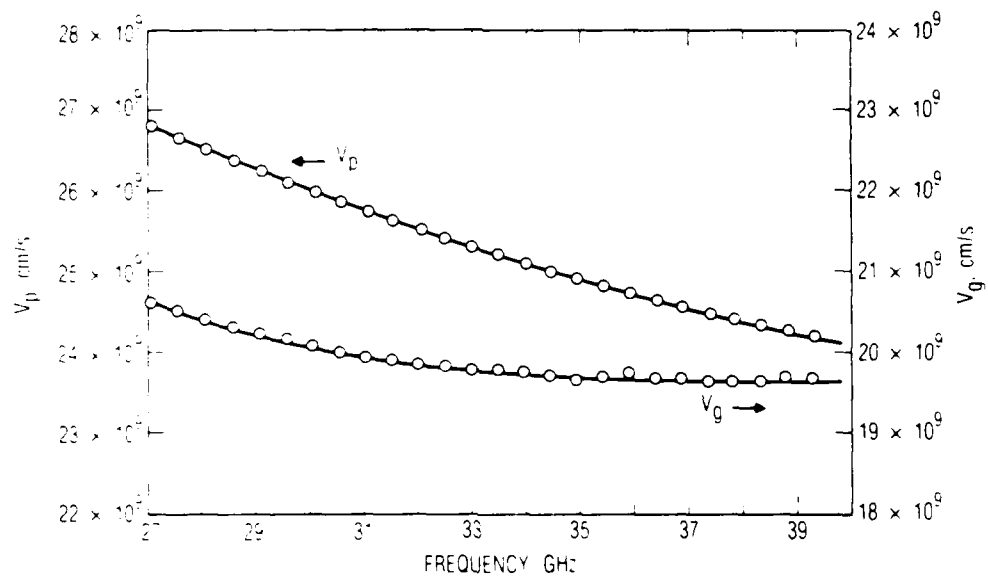


Fig. 8. Comparison of Measured and Calculated Group and Phase Velocities for a Teflon Rod Waveguide of Diameter 0.635 cm. The solid lines are calculated and the measurements are indicated by circles.

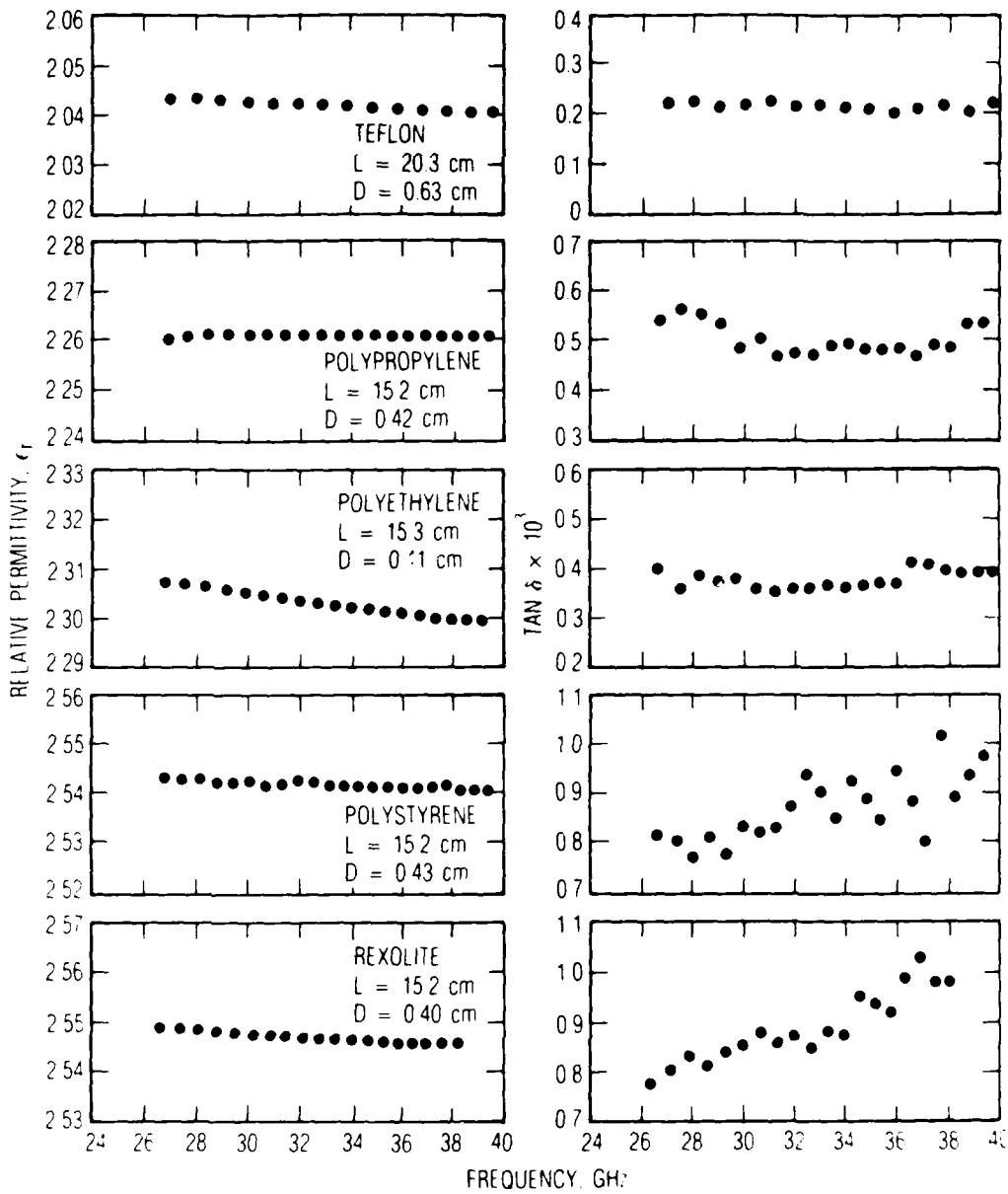


Fig. 9. Derived Values of  $\epsilon_r$  and  $\tan \delta$  from the Measurements for Different Dielectric Materials

brief discussion, including references, of alternate methods used to determine the complex permittivities of materials at the millimeter wavelengths has been given in Refs. 11 and 12. The corresponding attenuation coefficients for these dielectric waveguides are shown in Fig. 10. In Fig. 11 are plots of the half-power bandwidths at the different resonances for two lengths of 0.635-cm-diam Teflon waveguide. The plots indicate that the measured Q's are primarily due to the dielectric losses. If the wall losses were significant, the Q's of the shorter waveguide would have been noticeably lower at the lower frequencies and the derived loss tangents in Fig. 9 would have been noticeably higher. As a further check on the coupling effects, the insertion losses of the resonator system with a Teflon waveguide were measured at resonances near 27, 33, and 39 GHz. The measured insertion losses were -71, -63, and -51 dB, respectively, at these three frequencies.

Table 1. Measured Relative Permittivities and Loss Tangents, Ka-Band

Material	Estimates with Standard Error	
	$\epsilon_r$	$10^3 \tan\delta$
Teflon	2.0422±0.0006	0.217±0.006
Polypropylene	2.261±0.001	0.50±0.03
Polyethylene	2.302±0.003	0.38±0.02
Polystyrene	2.542±0.001	0.87±0.07
Rexolite	2.548±0.001	0.89±0.07

It is clear that for low-loss performance in circular dielectric waveguides, one should use small-diameter rods made from material with small relative permittivity and loss tangent. At the Ka-band the attenuation in a dielectric rod waveguide for small  $2a/\lambda_0$  can be less than that of a conventional rectangular metallic waveguide. Because the surface resistivity of metals is proportional to the square root of frequency, the losses in metallic

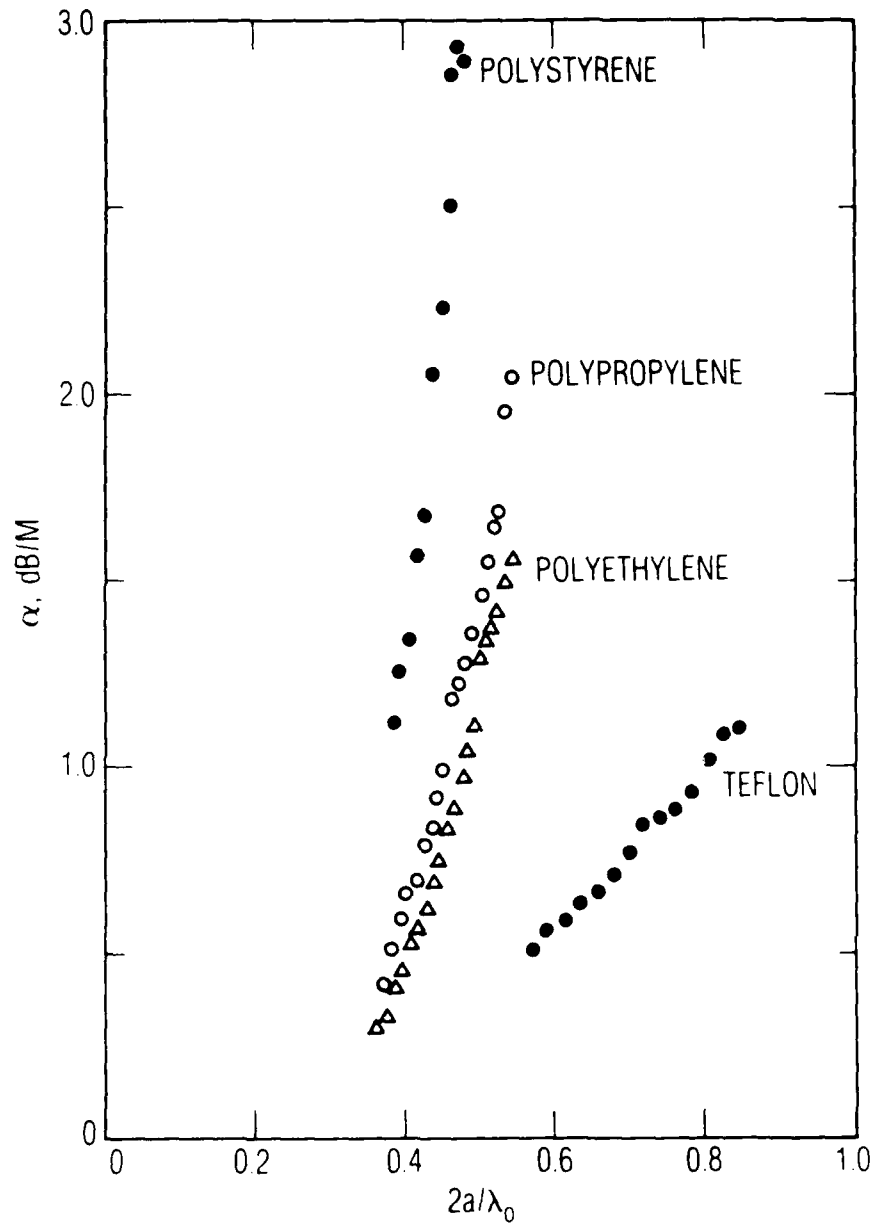


Fig. 10. Measured Attenuation Coefficients for the Different Dielectric Waveguides Corresponding to Fig. 9. Polystyrene and Rexolite have similar attenuation characteristics.

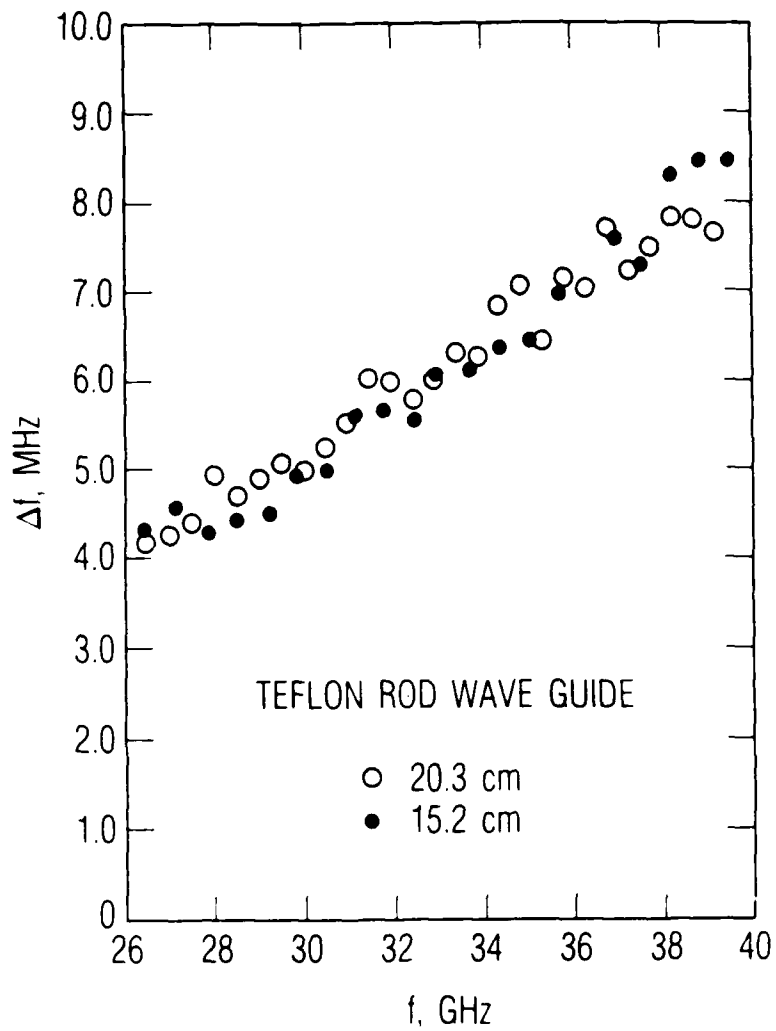


Fig. 11. Plot of Half-Power Transmission Bandwidths at the Different Resonances for Two Different Lengths (6 and 8 in.) of Circular Teflon Waveguide

waveguides increase with frequency relative to losses in dielectric waveguides. This is shown in Fig. 12, which plots the attenuation coefficients of different silver rectangular waveguides and of circular Teflon waveguides at the indicated frequencies. The assumption is that for the Teflon rod,  $2a/\lambda_0 = 0.4$  at the indicated frequencies. Since the attenuation coefficient of dielectric waveguides can be further reduced by using other than a circular cross section, dielectrics show promise as viable guiding structures at millimeter and submillimeter wavelengths.

To summarize, a resonator method, applicable at the millimeter and submillimeter wavelengths, that can accurately measure the attenuation coefficient of ultralow-loss dielectric waveguides has been described. In addition, the complex permittivity of the dielectric material of the waveguide can be derived. Since the fields are confined close to the dielectric core, long resonators can be conveniently implemented, permitting accurate measurements of  $\alpha$ ,  $\epsilon_r$ , and  $\tan\delta$ .

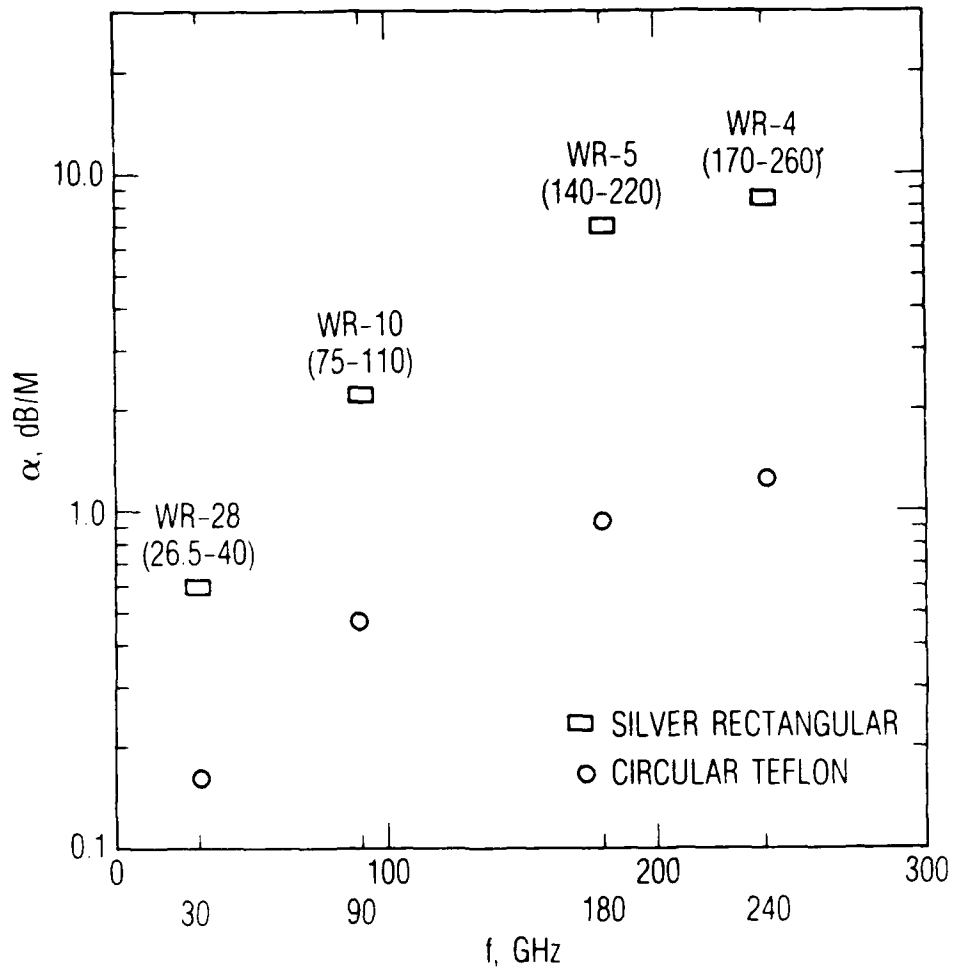


Fig. 12. Comparison of Attenuation Coefficients of Silver Rectangular and Teflon Circular Waveguides at the Indicated Frequencies. The waveguide range of the designated metal waveguides is shown in parentheses. For the dielectric waveguide, it is assumed that  $2a/\lambda_0 = 0.4$  at the indicated frequencies.

## REFERENCES

1. C. Chandler, "Investigation of Dielectric Rod as Waveguides," J. Appl. Phys. 20, 1188-1192 (1949).
2. J. R. Carson, S. P. Mead, and S. A. Schelkunoff, "Hyper-Frequency Waveguides--Mathematical Theory," Bell Syst. Tech. Journ. 15, 310-333 (1936).
3. C. Yeh, "Advances in Communication Through Light Fibers," in Advances in Communication Systems, Vol. 4, ed. A. Viterbi (Academic Press, Inc., New York, 1975).
4. S. Ramo, J. R. Whinnery, and T. Van Duzer, Fields and Waves in Communication Electronics, Second Edition (John Wiley, New York, 1984).
5. C. F. Davidson and J. C. Simmonds, "Cylindrical Cavity Resonators," Wireless Eng. 31 420-424 (1944).
6. H. M. Barlow and A. L. Cullen, Microwave Measurements (Constable and Company, Ltd., London, 1950).
7. D. D. King and S. P. Schlesinger, "Losses in Dielectric Image Lines," IRE Trans. Microwave Theory Tech. MTT-5, 31-35 (1957).
8. S. A. Schelkunoff, "The Impedance Concept and Its Application to Problems of Reflection, Refraction, Shielding, and Power Absorption," Bell Syst. Tech. Journ. 17, 17-48 (1938).
9. C. Yeh, "A Relation Between  $\alpha$  and Q," Proc. IRE 50, 2143 (1962).
10. C. Yeh, "Attenuation in a Dielectric Elliptical Cylinder," IEEE Trans. Ant. Prop. AP-11, 177-184 (1963).
11. M. N. Afsar, "Dielectric Measurements of Millimeter Wave Materials," IEEE Trans. Microwave Theory Tech. MTT-32, 1598-1609 (1984).
12. F. I. Shimabukuro, S. Lazar, M. R. Chernick, and H. B. Dyson, "A Quasi-Optical Method for Measuring the Complex Permittivity of Materials," IEEE Trans. Microwave Theory Tech. MTT-32, 659-665 (1984).